20. Metzner, A. B., "Advances in Heat Transfer," J. P. Hartnet and T. F. Irvine, Jr., ed., Academic Press, New York, pp. 357-374 (1965).
21. ———, R. D. Vaughn, and G. L. Houghton, *A.I.Ch.E. J.*, **3**, 92-100 (1957).
22. Oliver, D. R., and V. G. Jenson, *Chem. Eng. Sci.*, **19**, 115-129 (1964).
23. Peterson, A. W., Ph.D. thesis, Univ. Utah, Salt Lake City (1960).
24. Pigford, R. L., *Chem. Eng. Progr. Symp. Ser. No. 17*, **51**, 79 (1955).
25. Ree, T., and H. Eyring, *J. Appl. Phys.*, **25**, 793-809 (1955).
26. Reid, Robert C., and Thomas K. Sherwood, "Chemical Engineering Series," McGraw-Hill, New York (1958).
27. Salt, D. L., N. W. Ryan, and E. B. Christiansen, *J. Colloid. Sci.*, **6**, 2, 146-154 (1951).
28. Schenk, I., and J. Van Laar, *Appl. Sci. Res.*, **A7**, 449 (1958).
29. Schneider, P. J., *Trans. Am. Soc. Mech. Engrs.*, **79**, 765-773 (1957).
30. Tao, Fan-Sheng, M.S. thesis, Univ. Utah, Salt Lake City (1964).
31. Thomas, D. G., A.S.M.E. Second Symp. Thermophysical Properties, pp. 704-717, Academic Press, New York (1962).

Manuscript received April 4, 1966; paper accepted August 15, 1966. Paper presented at A.I.Ch.E. Detroit meeting.

The Effect of Recycle on a Linear Reactor

W. R. SCHMEAL and NEAL R. AMUNDSON

University of Minnesota, Minneapolis, Minnesota

The theoretical transient behavior of an isothermal packed bed or tubular reactor with direct recycle is investigated. It is shown that the recycle effect, coupled with the phenomenon of axial dispersion, causes waves in the reactant concentration to travel through the bed when the feed concentration undergoes a step change. The waves have a length almost equal to the bed length and they travel with the velocity of the fluid. The behavior of the waves is very insensitive to the value of the Peclet number.

The pertinent linear differential equation is solved by the method of generalized Fourier transforms and the boundary conditions are such that the Sturm-Liouville theorem cannot be used. The operator is nonself-adjoint and the eigenfunctions are not mutually orthogonal. The eigenvalues, which are complex, are found by means of the argument principle. Sample calculations are presented of the first one hundred terms of the Fourier expansion of a solution function and this is compared to a simplified approximate series which is developed.

Recycle streams are often employed with packed beds or tubular reactors for temperature control, inhibition of undesired side reactions, or efficient use of reactants. Recycling effects feed back of information from the reactor exit to the entrance. This may couple with the phenomenon of axial dispersion that provides communication throughout the fluid, and aggravate or reenforce instabilities.

How a step change in feed concentration of reactant effects damped oscillations in the concentration profile within the bed is shown here for the relatively simple case of an isothermal reactor with a first-order reaction occurring. For mathematical simplicity the case of direct recycle is considered, the method being amenable to the inclusion of a linear process or time lag in the recycle stream. In actual practice, fractionation and heat exchange processes may be present in the recycle stream which are complicated to analyze and have a strong effect on the stability of the system. The example chosen should however give qualitative information about the dynamics of other processes which incorporate recycle, such as polymerization reactors and crystallizers (*8*).

The law of conservation of mass applied to the isothermal flow reactor produces a linear differential equation for the concentration of reactant c as a function of time t and of axial position x.

$$D\frac{\partial^2 c}{\partial x^2} - u\frac{\partial c}{\partial x} - kc = \frac{\partial c}{\partial t} \tag{1}$$

The term on the left represents a diffusive flux of reactant, the second a convective flux, and the last a volumetric rate of depletion via reaction, while the term on the right accounts for the local accumulation rate.

The form of the equation is

$$L(c) = \partial c/\partial t \tag{2}$$

W. R. Schmeal is with Shell Development Company, Emeryville, California.

This equation, when considered with the Danckwerts boundary condition (*4*) for the special case of no recycle, is essentially a Sturm-Liouville system (*10*). The operator in x, $L(\ )$, may be made self-adjoint, and its eigenvalues in this new format may be shown to be real by the Sturm-Liouville theorem. The associated eigenfunctions are therefore orthogonal and it is not difficult to construct the solution to Equation (1) for a step change in feed concentration by separation of variables or the method of generalized Fourier transforms (*2*). Although the convergence of the resultant infinite series is slow, calculations are not difficult, because the eigenvalues are real and almost periodic and may be found by a simple numerical scheme.

PRELIMINARY ANALYSIS AND SOLUTION

When recycle is considered, the boundary conditions pertinent to Equation (1) or (2) become "mixed"—the exit conditions affect the feed. This precludes the application of the Sturm-Liouville theorem to the system. The operator $L(\ )$ becomes nonself-adjoint because a different set of boundary conditions is associated with its adjoint. The eigenfunctions of $L(\ )$ are not orthogonal to one another and the eigenvalues will be shown to be complex in general. A real infinite series solution to Equation (1) evolves however because the terms occur in complex conjugate pairs.

The Danckwerts boundary conditions will be used. For direct recycle with no time lag and for constant feed concentration c_F, the boundary and initial conditions are

$$(1-R)c_F = c(0,t) - R\,c(l,t) - D\frac{\partial c}{\partial x}(0,t), \quad t>0 \tag{3}$$

$$\frac{\partial c}{\partial x}(l,t) = 0 \quad , t>0$$

$$c(x,0) = c_o(x) \quad , 0<x<l$$

The system (1) and (3) may be made dimensionless, and the boundary conditions homogeneous by the variable change

$$y = \frac{c-c_F}{c_F} \quad z = \frac{x}{l} \quad \theta = \frac{tu}{l} \quad Da = \frac{kl}{u} \quad B_o = \frac{ul}{D} \tag{4}$$

This change yields the system

$$\frac{1}{Bo}\frac{\partial^2 y}{\partial z^2} - \frac{\partial y}{\partial z} - Da\,y - Da = \frac{\partial y}{\partial \theta} \tag{5}$$

$$y(0,\theta) - R\,y(1,\theta) - \frac{1}{Bo}\frac{\partial y}{\partial z}(0,\theta) = 0 \quad \theta>0$$

$$\frac{\partial y}{\partial z}(1,\theta) = 0 \qquad \theta > 0$$

$$y(z,0) = y_o(z) \qquad 0<z<1$$

The differential equation is of the form

$$\mathcal{L}(y) - Da = \frac{\partial y}{\partial \theta} \tag{6}$$

Its solution, constructed by the method of generalized Fourier transforms, is

$$y(z,\theta) = \sum_{i=0}^{\infty}\left\{\left[\int_o^1 y_o(\zeta)\,U_i^*(\zeta)d\zeta + \frac{\int_o^1 Da\,U_i^*(\zeta)d\zeta}{\eta_i}\right]e^{-\eta_i\theta} - \frac{\int_o^1 Da\,U_i^*(\zeta)d\zeta}{\eta_i}\right\}$$

$$\frac{\psi_i(z)}{\int_o^1 \psi_i(\zeta)\,U_i^*(\zeta)d\zeta} \tag{7}$$

where * denotes complex conjugate.

The $\{\eta_i\}$ are the eigenvalues of $\mathcal{L}(\ )$ and the $\{\psi_i(z)\}$ are its eigenfunctions. The $\{U_i(z)\}$ are the adjoint eigenfunctions of $\mathcal{L}(\ )$, solutions to

$$\mathcal{L}_a(U_i) = -\,\eta_i^*\,U_i \tag{8}$$

Here, $\mathcal{L}_a(\ )$ is the adjoint operator to $\mathcal{L}(\ )$, defined by Green's formula, and the boundary conditions appropriate to (8) are those compatible with the bilinear concommitant (*6*). Each $U_i(z)$ is orthogonal to every $\psi_i(z)$ except those associated with its own eigenvalue η_i (*3*).

For any second-order linear differential operator, it is always possible to find a change of dependent variable which renders the operator the same as its adjoint (*6*). Although the change cannot make the problem self-adjoint, because of the boundary conditions, it is employed here to simplify computations. Define $Y(z)$ by

$$Y(z) = e^{-\frac{Bo\,z}{2}}\,y(z) \tag{9}$$

This substitution made in the system (5) or (6) altets the differential equation and its boundary conditions. The former is of the form

$$\mathcal{L}^{sa}(Y) - Da\;e^{-\frac{Bo\,z}{2}} = \frac{\partial Y}{\partial \theta} \tag{10}$$

where

$$\mathcal{L}^{sa}(\ ) = \frac{1}{Bo}\frac{\partial^2}{\partial z^2} - \left(\frac{Bo}{4} + Da\right)$$

The solution of this new system may be formed by multiplying Equation (7) through by exp $(-Bo\ z/2)$. The eigenfunctions $\{\psi_i^{sa}(z)\}$ and adjoint eigenfunctions $\{U_i^{sa}(z)\}$ of the operator $\mathcal{L}^{sa}(\ )$ are related to those of $\mathcal{L}(\ )$ by (*9*)

$$\psi_i(z) = e^{\frac{Bo\,z}{2}}\,\psi_i^{sa}(z)$$

$$U_i(z) = e^{-\frac{Bo\,z}{2}}\,U_i^{sa}(z) \tag{11}$$

The eigenvalues $\{\eta_i\}$ for problems (6) and (10) are the same (*9*).

It is convenient to make a transformation concerning the eigenvalues

$$\xi_i^2 = Bo\left(\eta_i - \frac{Bo}{4} - Da\right) \tag{12}$$

The eigenproblem is simplified to

$$\frac{\partial^2\psi_i^{sa}}{\partial z^2} = -\,\xi_i^2\,\psi_i^{sa} \tag{13}$$

Examination of the compatibility of the solutions of this equation to the boundary conditions shows that the $\{\xi_i\}$ must be roots of

$$g(\xi_i) = \left(1 - \frac{4}{Bo^2}\xi_i^2\right)\sin\xi_i + \frac{4}{Bo}\xi_i\cos\xi_i - \frac{4}{Bo}\xi_i\,e^{\frac{Bo}{2}}\,R = 0 \tag{14}$$

The eigenfunctions may be expressed in several forms through manipulations using Equation (14). One of these is

$$\psi_i^{sa}(z) = \frac{Bo}{2} \sin \xi_i (1 - z) + \xi_i \cos \xi_i (1 - z) \quad (15)$$

The adjoint eigenfunctions are

$$U_i^{sa}(z) = \frac{Bo}{2} \sin \xi_i^* z + \xi_i^* \cos \xi_i^* z \quad (16)$$

It remains only to find the eigenvalues, the zeroes of (14), to be able to evaluate the solution function given by Equation (7).

CHARACTER OF THE EIGENVALUES

It will be shown that the roots of $g(\xi)$ are complex in general. These eigenvalues fall near two conjugate curves in the complex plane, symmetric to each other about the real axis and each symmetric about the imaginary axis. These curves are denoted $z(Bo, R, \hat{x}, \hat{y})$ and $z(Bo, R, \hat{x}, \hat{y}^*)$ where

$$\hat{x} = Re\, \xi$$

$$\hat{y} = Im\, \xi$$

These curves, shown in Figure 1, become one real line for

$$|\hat{x}| > Bo\, (Re^{Bo/2} - 1) \quad (17)$$

The group Bo, defined by (4), generally has a value greater than ten, and $0 \leq R \leq 1$. When there is no recycle ($R = 0$) the eigenvalues adhere to the Sturm-Liouville theorem and all are real.

For $R > 0$, increases in R or Bo affect the curve $z(Bo, R, \hat{x}, \hat{y})$ in such a manner that the two smallest positive real eigenvalues approach one another. Upon intersecting these two eigenvalues leave the real axis for increases in R or Bo and become complex conjugates of each other. Then the next pair approach one another. The intersection of two eigenvalues in this fashion represents a root of the first derivative of $g(\xi)$ as well as a root of $g(\xi)$ itself.

Such second-order eigenvalues have the property that the corresponding eigenfunction and adjoint eigenfunction are orthogonal. In this case the eigenfunctions do not form a complete set in the space of continuous functions. This is apparent because the adjoint eigenfunction belonging to the above eigenvalue is orthogonal to every eigenfunction.

This pathological situation may be rectified by the construction of an auxiliary function $d\psi/d\xi$ which completes

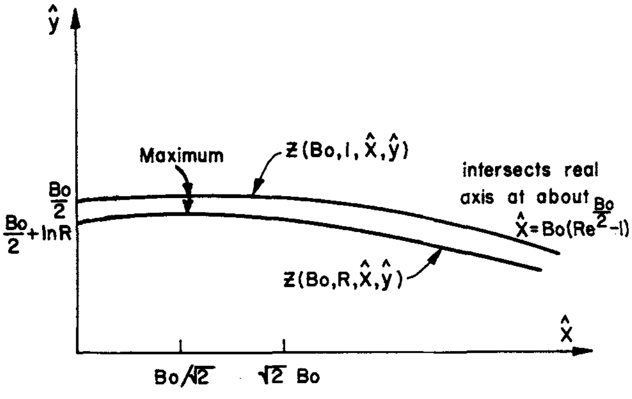

Fig. 1. Behavior of the eigencurve $z(Bo, R, \hat{x}, \hat{y})$ in the ξ plane for two values of recycle ratio, 1 and R.

the set of eigenfunctions (9). However, this event of incompleteness occurs only for isolated values of Bo and R and the expansion (7) is valid for all other values.

The curves z lie in a domain in the ξ plane which maps into the right half of the η plane. The η plane is described by the transformation inverse to (12)

$$\eta(\xi) = \frac{Bo}{4} + Da + \frac{\xi^2}{Bo} \quad (18)$$

Thus, for all eigenvalues

$$Re(-\eta) < 0 \quad (19)$$

This implies stability of the reactor in the sense that the function $Y(z, \theta)$ decays in time to the steady state $Y_{ss}(z)$ for constant feed composition.

For $R > 0$ the smallest fifty or sixty eigenvalues will be shown to be approximated closely by

$$\hat{x}_n = \pm\, 2\pi n \qquad n = 0, 1, 2 \ldots$$

$$\hat{y}_n = \pm \left(\frac{Bo}{2} + \ln R \right) \quad (20)$$

APPLICATION OF THE ARGUMENT PRINCIPLE

The eigenequation (14) has two symmetry properties which may be utilized immediately. They are

$$g(\xi) = -\, g(-\xi) \quad (21)$$

and

$$g(\xi) = g^*(\xi^*) \quad (22)$$

The first follows from a direct substitution of $-\xi$ into $g(\xi)$. This implies that if ξ_i is a root of $g(\xi)$, so is $-\xi_i$. Since both ξ_i and $-\xi_i$ map onto the same η_i by transformation (18), it is satisfactory to consider only ξ_i with positive real parts.

The second property is the reflection property (*1*) of analytic functions, which implies that if $g(\xi)$ is real for real ξ then (22) holds. The converse is also true. This property implies that if ξ_i is an eigenvalue, so is its complex conjugate ξ_i^*. It will be necessary to search for eigenvalues with non-negative imaginary parts only.

The argument principle of complex variable theory (5) will be used to show that there are two eigenvalues whose real parts are bounded by

$$2\pi N + \pi < \hat{x} < 2\pi N + 3\pi \quad (23)$$

for each real integer N except $N = -1$. Second, the distribution of eigenvalues in subintervals of these intervals will be determined.

The analytic function $g(\xi)$ has no poles or other singularities in the finite complex plane. Therefore the argument principle determines that the number of zeroes of $g(\xi)$ within any curve in the ξ plane is the number of revolutions about the origin made by the mapping of this curve in the $g(\xi)$ plane.

The real and imaginary parts of $g(\xi)$ are

$$Re\, g(\xi) = Re(\hat{x}, \hat{y}) = \left[1 + \frac{4}{Bo^2} (\hat{y}^2 - \hat{x}^2) \right] \sin \hat{x} \cosh \hat{y} + \frac{8}{Bo^2} \hat{x}\hat{y} \cos \hat{x} \sinh \hat{y} + \frac{4}{Bo} \hat{x} \cos \hat{x} \cosh \hat{y} + \frac{4}{Bo} \hat{y} \sin \hat{x} \sinh \hat{y} - \frac{4R}{Bo} \hat{x}\, e^{Bo/2} \quad (24)$$

and

$$Im\, g(\xi) = Im(\hat{x}, \hat{y}) = \left[1 + \frac{4}{Bo^2} (\hat{y}^2 - \hat{x}^2) \right] \cos \hat{x} \sinh \hat{y}$$

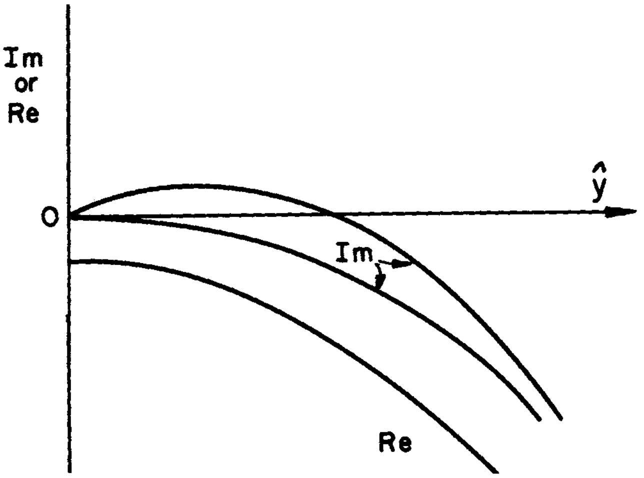

Fig. 2. Typical curves of *Re* and *Im*, the real and imaginary parts of $g(\xi)$, vs. $\hat{y} = Im\xi$ for $x = Re\xi = \pi + 2\pi N$ (N is a positive integer).

$$-\frac{8}{Bo^2}\hat{x}\hat{y}\sin\hat{x}\cosh\hat{y} - \frac{4}{Bo}\hat{x}\sin\hat{x}\sinh\hat{y} + \frac{4}{Bo}\hat{y}\cos\hat{x}\cosh\hat{y} - \frac{4R}{Bo}\hat{y}\,e^{Bo/2} \quad (25)$$

If the real part of ξ is the lower bound appearing in (23), $\hat{x} = \pi + 2\pi N$; then

$$\sin\hat{x} = 0 \qquad \cos\hat{x} = -1$$

The real and imaginary parts of $g(\xi)$ simplify to

$$Re(\hat{x}, \hat{y}) = -\frac{4}{Bo}\hat{x}\left(\cosh\hat{y} + \frac{2\hat{y}}{Bo}\sinh\hat{y}\right) - \frac{4R}{Bo}e^{Bo/2}\hat{x} \quad (26)$$

and

$$Im(\hat{x}, \hat{y}) = -\left[1 - \frac{4}{Bo^2}(\hat{x}^2 - \hat{y}^2)\right]\sinh\hat{y} - \frac{4}{Bo}\hat{y}\cosh\hat{y} - \frac{4R}{Bo}\hat{y}\,e^{Bo/2} \quad (27)$$

Typical curves of $Re(\pi + 2\pi N, \hat{y})$ and $Im(\pi + 2\pi N, \hat{y})$ for $\hat{y} \geqq 0$ and $N \geqq 0$ are sketched in Figure 2. The important point to note is that $Re(\hat{x}, \hat{y})$ is always negative for these values of $\hat{x}$ and $\hat{y}$. This implies that a ray in the ξ plane beginning on the real axis at $\hat{x} = \pi + 2\pi N$, ($N \geqq 0$) and proceeding in a positive imaginary direction maps into a curve in the $g(\xi)$ plane, every point of which has a negative real part.

Next a line segment will be constructed in the ξ plane perpendicular to the rays described above and intersecting at least two of them. This line will consist of points all of which have the same large positive imaginary part. Let $\hat{y} = \hat{y}_o >> Bo/2$ where in addition, $\hat{y}_o >> \hat{x}$.

For these large values of $\hat{y}$, $g(\xi)$ simplifies to

$$Re(\hat{x}, \hat{y}_o) \approx \left[\frac{4}{Bo^2}\hat{y}_o^2\sin\hat{x} + \frac{8}{Bo^2}\hat{x}\hat{y}_o\cos\hat{x}\right]e^{\hat{y}_o} - \frac{4R}{Bo}\hat{x}\,e^{Bo/2} \quad (28)$$

and

$$Im(\hat{x}, \hat{y}) \approx \left[\frac{4}{Bo^2}\hat{y}_o^2\cos\hat{x} - \frac{8}{Bo^2}\hat{x}\hat{y}_o\sin\hat{x}\right]e^{\hat{y}_o} - \frac{4R}{Bo}\hat{y}_o\,e^{Bo/2} \quad (29)$$

The first of these, $R(\hat{x}, \hat{y}_o)$, behaves like $\sin\hat{x}$ with a large amplitude, while $Im(\hat{x}, \hat{y}_o)$ resembles $\cos\hat{x}$ with a large amplitude. Over an interval in $\hat{x}$ of length 2π, these two functions describe a circlelike curve in the $g(\xi)$ plane whose center lies closer to the zero point than does any point belonging to the curve. Although the distance between $g(\hat{x} + i\hat{y}_o)$ and $g(\hat{x} + 2\pi + i\hat{y}_o)$ is on the order of $16\pi\, y_o\, e^{\hat{y}_o}/Bo^2$, this is not large compared to $|(g(\hat{x} + i\hat{y}_o)|$.

From Equations (26) through (29) a mapping may be made in the $g(\xi)$ plane of the following curve, called Γ, which is in the ξ plane.

$$\Gamma = \{\xi = \hat{x} + i\hat{y} \mid \hat{x} = \pi + 2\pi N,\ 0 \leqq \hat{y} \leqq \hat{y}_o \quad (30)$$

and

$$\pi + 2\pi N \leqq \hat{x} \leqq 3\pi + 2\pi N,\ \hat{y} = \hat{y}_o\}$$

This curve and its mapping are shown in Figure 3. Equations (26) and (27) may be used again to construct a line segment in the ξ plane from $(3\pi + 2\pi N + i\hat{y}_o)$ perpendicular to the real axis. Then the reflection property of the mapping, Equation (22), which states that a point and its conjugate map into a point and its conjugate, may be utilized to complete the mapping of a rectangle. The resultant transformation is shown in Figure 4.

The number of revolutions about the origin of the mapping in the $g(\xi)$ plane of the rectangle is always two.

Therefore within every interval N of the ξ plane characterized by

$$\pi + 2\pi N < Re\,\xi = \hat{x} < 3\pi + 2\pi N$$

lie either two eigenvalues or one. N may be any positive or negative integer, except -1. If there is only one eigenvalue ξ_i in an interval, it satisfies

$$\frac{dg(\xi_i)}{d\xi} = g(\xi_i) = 0 \quad (31)$$

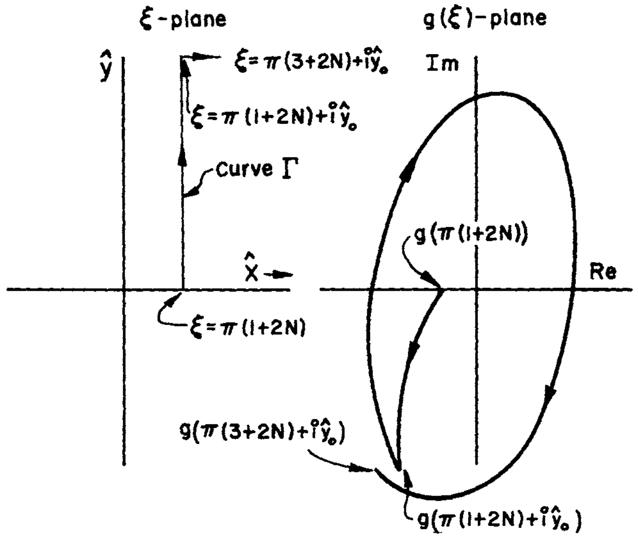

Fig. 3. Typical mapping in the $g(\xi)$ plane of the curve Γ in the ξ plane.

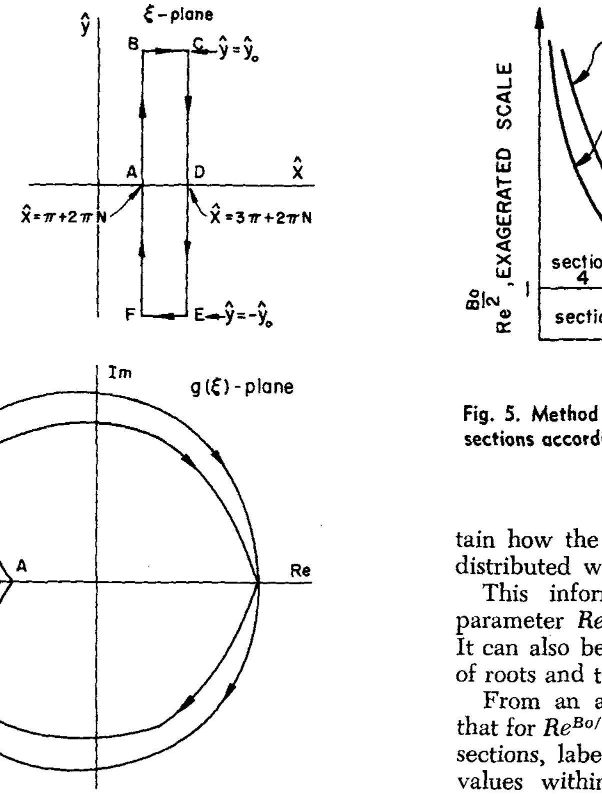

Fig. 4. Typical mapping in the $g(\xi)$ plane of the rectangle in the ξ plane.

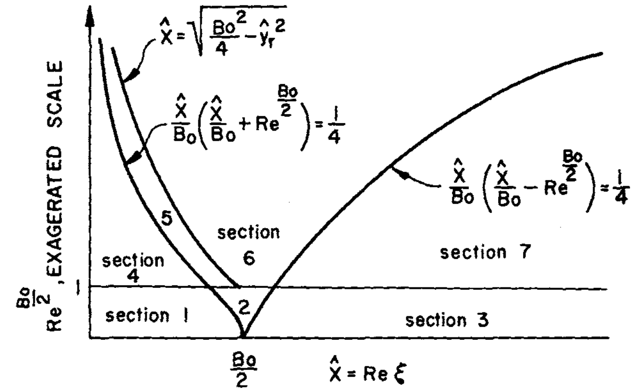

Fig. 5. Method of dividing positive real axis of ξ plane into seven sections according to distribution of roots of $g(\xi)$. $Re^{Bo/2}$ determines the dividing lines.

and

$$\frac{d^2g(\xi_i)}{d\xi^2} \neq 0$$

Furthermore if there is only one eigenvalue it is real, since complex roots of $g(\xi)$ occur in conjugate pairs.

The eigenvalues have thus been established to be countable. Furthermore they may be ordered in terms of increasing positive real part. This information about the approximate location of the roots of $g(\xi)$ may be incorporated in a numerical scheme to find their exact location.

FURTHER INFORMATION FROM THE ARGUMENT PRINCIPLE

The rectangles in the ξ plane shown in Figure 4 may be divided into four subrectangles of equal area by constructing three line segments perpendicular to the real axis. The argument principle may again be used to ascertain how the two eigenvalues in the larger rectangle are distributed within these subrectangles.

This information reveals, in rough form, how the parameter $Re^{Bo/2}$ affects the location of the eigenvalues. It can also be used to prove postulates about the location of roots and to corroborate other calculations.

From an analysis of this type, it may be shown (9) that for $Re^{Bo/2} < 1$, the real axis can be divided into three sections, labelled 1, 2, and 3. The distribution of eigenvalues within the subrectangles for a rectangle lying wholly in one of these sections is shown in Table 1. The value of $\hat{x} = Re\ \xi$ at which these sections begin and end is shown in Figure 5 for values of the parameter, $Re^{Bo/2}$. Also shown in Figure 5 is the location of the sections for $Re^{Bo/2} > 1$. There are four of these sections labelled 4, 5, 6, and 7, and the distribution of eigenvalues into the subrectangles in these sections is shown in Table 2. In Figure 5, $\hat{y}_r$ is a root of

$$\frac{2}{Bo}\hat{y}_r \sinh \hat{y}_r + \cosh \hat{y}_r - Re^{Bo/2} = 0$$

From the above it may be seen that for $Re^{Bo/2} < 1$, the eigenvalues are always real, since complex roots must occur in pairs. Table 1 indicates that there can be no pairs for $Re^{Bo/2} < 1$.

When $Re^{Bo/2} > 1$, Figure 5 indicates that the smallest roots may be real, the two falling into different subrectangles. Actually section 4 is so small in length that no roots could possibly lie in it unless $R \approx e^{-Bo/2}$. The roots in rectangles in sections 5 and 6 may be complex, since the pairs occur in the same subrectangles. If

TABLE 1

	Section 1	Section 2	Section 3
Roots in subinterval 1 $(\pi + 2\pi N < \hat{x} < 3\pi/2 + 2\pi N)$	0	0	1
Roots in subinterval 2 $(3\pi/2 + 2\pi N < \hat{x} < 2\pi + 2\pi N)$	1	1	0
Roots in subinterval 3 $(2\pi + 2\pi N < \hat{x} < 5\pi/2 + 2\pi N)$	0	1	1
Roots in subinterval 4 $(5\pi/2 + 2\pi N < \hat{x} < 3\pi + 2\pi N)$	1	0	0

TABLE 2

	Section 4	Section 5	Section 6	Section 7
Roots in subinterval 1 $(\pi + 2\pi N < \hat{x} < 3\pi/2 + 2\pi N)$	0	0	0	1
Roots in subinterval 2 $(3\pi/2 + 2\pi N < \hat{x} < 2\pi + 2\pi N)$	0	0	2	1
Roots in subinterval 3 $(2\pi + 2\pi N < \hat{x} < 5\pi/2 + 2\pi N)$	1	2	0	0
Roots in subinterval 4 $(5\pi/2 + 2\pi N < \hat{x} < 3\pi + 2\pi N)$	1	0	0	0

$$\hat{x} > \frac{Bo\, Re^{Bo/2} + Bo\sqrt{R^2 e^{Bo} + 1}}{2} \quad (32)$$

the rectangle lies in section 7 and the eigenvalues must be real. Actually, it may be shown (9) from inspection of the eigenequation (14) that if $\hat{x}_i$ is a positive real eigenvalue

$$\hat{x}_i \geqq Bo\,(Re^{Bo/2} - 1) \quad (33)$$

The mapping of the curve Γ given by Equation (30) and shown in Figure 3 can be used to show that only one eigenvalue exists in the interval $-\pi \leqq \hat{x} \leqq \pi$. These eigenvalues are zero and $\pm\, i\left(\frac{Bo}{2} + \ln R\right)$ if $Re^{Bo/2}$ is sufficiently large.

THE EIGENVALUE CURVE

A curve $z(Bo, R, \hat{x}, \hat{y})$ may be generated in the ξ plane near which eigenvalues are constrained to fall. It is found by expressing the eigenequation as

$$\left(1 - \frac{4\xi^2}{Bo^2}\right)\sin\xi + \frac{4\xi}{Bo}\cos\xi = -\frac{4R}{Bo}\,\xi\, e^{Bo/2} \quad (34)$$

If ξ satisfies this, the absolute value of the left and right sides of this equation are equal. For $\hat{y} > 3$ the absolute value of the left side may be approximated by

$$\frac{2}{Bo^2}\, e^{\hat{y}}\left[\hat{x}^2 + \left(\hat{y} + \frac{Bo}{2}\right)^2\right]$$

The following curve is thus established:

$$2R\,Bo\,e^{Bo/2}\sqrt{\hat{x}^2 + \hat{y}^2} = e^{\hat{y}}\left[\hat{x}^2 + \left(\hat{y} + \frac{Bo}{2}\right)^2\right] \quad (35)$$

These curves are sketched in Figure 1 for a general value of R ($0 < R < 1$) and for a unit value of R. They have the property that (9)

$$\hat{y}(\hat{x}, R) \approx \hat{y}(\hat{x}, 1) + \ln R \quad (36)$$

Thus, it is only necessary to investigate the curve for a recycle ratio of unity. $z(Bo, 1, \hat{x}, \hat{y})$ intersects the $\hat{y}$ axis at $\hat{y} = Bo/2$. It resembles the straight line $\hat{y} = Bo/2$ for $0 < \hat{x} < \sqrt{2}\,Bo$, passing through the point $(\hat{x}, \hat{y}) = (\sqrt{2}\,Bo, Bo/2)$. It actually has a small positive slope for $0 < \hat{x} < Bo/\sqrt{2}$, reaching a maximum value of $\hat{y}$ at $\hat{x} = Bo/\sqrt{2}$. This maximum $\hat{y}$ can be shown to be less than $Bo/2 + \ln(4/3)^{1/2}$ (9).

For $\hat{x} > \sqrt{2}\,Bo$, the curve $z(Bo, 1, \hat{x}, \hat{y})$ has a negative slope, $\hat{y}$ decreasing logarithmically. For very large $\hat{x}$ (and $\hat{y} > 3$, say)

$$\hat{y} \approx \frac{Bo}{2} - \ln\frac{\hat{x}}{2Bo} \quad (37)$$

The curve intersects the $\hat{x}$ axis near $\hat{x} = Bo(e^{Bo/2} - 3)$ as indicated by Equation (33).

It is apparent, then, from the location of these curves in the complex plane that the eigenvalues of smaller magnitude have imaginary parts given approximately by

$$Im\,\xi_i = \hat{y}_i \approx \frac{Bo}{2} + \ln R \quad (38)$$

LOCATION OF THE SMALLER EIGENVALUES

The location of the eigenvalues lying on the curve $z(Bo, R, \hat{x}, \hat{y})$ may be found by eliminating the parameter R from the two expressions for the real and imaginary parts of $g(\xi)$, (24) and (25). Use of the approximations $\sinh\hat{y} = \cosh\hat{y} = \frac{1}{2}e^{\hat{y}}$ yields the single equation

$$\left[\left(\frac{4\hat{y}}{Bo^2} + \frac{4}{Bo}\right)\hat{x}^2 + \hat{y} + \frac{4\hat{y}^2}{Bo} + \frac{4\hat{y}^3}{Bo^2}\right]\sin\hat{x} = \left[-\frac{4\hat{x}^3}{Bo^2} + \left(1 - \frac{4\hat{y}^2}{Bo^2}\hat{x}\right)\right]\cos\hat{x} \quad (39)$$

$\hat{y}$ may be eliminated from this by means of Equation (38), the expression for the curve $z(Bo, R, \hat{x}, \hat{y})$. The resultant function of $\hat{x}$ may be plotted to find its zeroes.

It is a necessary but not sufficient condition that a complex eigenvalue have a real part satisfying this equation. In fact, it may be shown that there are two solutions in every interval, $\pi + 2\pi N \leqq \hat{x} \leqq 3\pi + 2\pi N$ ($N \geqq 0$). However the argument principle indicated that there are two eigenvalues in this interval but if complex they must have the same real part. Thus half of the values of $\hat{x}$ determined by the above procedure do not correspond to the real part of an eigenvalue.

The analysis of the distribution of eigenvalues into subrectangles using the argument principle summarized in Table 2 showed that the real part of complex eigenvalues satisfy either

$$\frac{3\pi}{2} + 2\pi N < \hat{x} < 2\pi + 2\pi N \quad (40)$$

or

$$2\pi + 2\pi N < \hat{x} < \frac{5\pi}{2} + 2\pi N$$

This determines which solutions to Equation (39) are spurious and which are real parts of eigenvalues.

It happens that those solutions of Equation (39) that represent real parts of eigenvalues are close to being multiples of 2π. This approximation becomes worse as $\hat{x}$ increases. Thus the first approximation to the smaller eigenvalues is

$$\xi_N = \pm\, 2\pi N \pm i\left(\frac{Bo}{2} + \ln R\right),\quad N = 0, 1, 2 \ldots \quad (41)$$

The smallest 100 eigenvalues were found by a Newton-Raphson (7) numerical procedure with (41) used as an initial guess. Various recycle ratios R were used between 10^{-5} and 0.99999, while a value of Bo (Peclet number with the bed length used as the length parameter) of 666.7 was assumed. No more than five trials were needed to produce ξ_N whose real and imaginary parts differed from the previous trial by less than 10^{-7}. In general these roots were well within 1% of the initial guesses, Equation (41).

The following representative eigenvalues, found numerically, indicate the accuracy of Equation (41) over a wide range of recycle ratios, R. With $R = 10^{-5}$ ($\ln R = -11.5$)

$$\xi_1 = \pm\, 6.284 \pm i\,(321.8) = \pm\, 6.284 \pm i\left(\frac{Bo}{2} - 11.51\right)$$

$$\xi_{100} = \pm 627.9 \pm i\,(322.0) = \pm 627.9 \pm i\left(\frac{Bo}{2} - 11.38\right)$$

With $R = 0.9999$

$$\xi_1 = \pm 6.283 \pm i\,(333.3) = \pm 6.283 \pm i\left(\frac{Bo}{2} + 7.88 \times 10^{-5}\right)$$

$$\xi_{100} = \pm 627.9 \pm i\,(333.5) = \pm 627.9 \pm i\left(\frac{Bo}{2} + 0.1222\right)$$

CALCULATIONS

The character and approximate location of the eigenvalues having been established, it is possible to evaluate the transient reactant concentration profiles given by (7). The steady state profiles are obtained by allowing θ to become infinite. That is

$$y_{ss}(z) = -\sum_{i=0}^{\infty} \frac{\int_0^1 Da\, U_i^*(\zeta)\, d\zeta}{\eta_i} \frac{\psi_i(z)}{\int_0^1 \psi_i(\zeta)\, U_i^*(\zeta)\, d\zeta} \tag{42}$$

Equation (7) may thus be rewritten as

$$y(z, \theta) = y_{ss}(z) + \sum_{i=0}^{\infty} \frac{\int_0^1 \left[y^o(\zeta) + \frac{Da}{\eta_i} \right] U_i^*(\zeta)\, d\zeta}{\int_0^1 \psi_i(\zeta)\, U_i^*(\zeta)\, d\zeta} \psi_i(z)\, e^{-\eta_i\theta} \tag{43}$$

This transient consists of the steady state profile plus a function which decays away in time. Initially this decaying function is the initial condition minus the steady state.

The steady state function must satisfy Equation (5) with the accumulation term removed. The solution to this ordinary differential equation is

$$y_{ss}(z) = -1 + \frac{(1-R)\, e^{Boz/2}}{\Delta} \left[\left(\frac{Bo}{2} + \sqrt{\gamma}\right) e^{\sqrt{\gamma}\,(1-z)} - \left(\frac{Bo}{2} - \sqrt{\gamma}\right) e^{-\sqrt{\gamma}\,(1-z)} \right] \tag{44}$$

where

$$\Delta = \left[Bo\left(\frac{1}{2} - R\, e^{Bo/2 - \sqrt{\gamma}}\right) + \frac{2\gamma}{Bo} \right] \cosh\sqrt{\gamma} + \sqrt{\gamma}\,[2 - 2R\, e^{Bo/2 - \sqrt{\gamma}}] \sinh\sqrt{\gamma}$$

and

$$\gamma = Bo\left(\frac{Bo}{4} + Da\right)$$

Plots of $c(z)/c_F$ obtained from the above equation are shown in Figure 6 for various recycle ratios R and $Da = 1$. Calculations were made with values of Bo of 666.67, 1,000, and infinity (no diffusion) used. The profiles are so insensitive to this Peclet number that the plots for different values of Bo are indistinguishable. (The criterion that $y_{ss}(z)$ be insensitive to Bo is that $2Da/Bo << 1$.)

The infinite series (42) is equivalent to the steady state function (44). The expansion (43) should give good convergence for times θ greater than zero, however. Each term in (43) decays in time like $e^{-\eta_i\theta}$, and the real part of η_i is large and positive for the larger eigenvalues. To evaluate (43) it is necessary to calculate the decaying function of the steady state which appears in $y(z, \theta)$. This is

$$y_D(z, \theta) = \sum_{i=0}^{\infty} \frac{\int_0^1 Da\, U_i^*(\zeta)\, d\zeta}{\eta_i \int_0^1 \psi_i(\zeta)\, U_i^*(\zeta)\, d\zeta} \psi_i(z)\, e^{-\eta_i\theta} \tag{45}$$

For ease of manipulation, it is convenient to carry out the calculations for this function in the self-adjoint format, that is, in terms of $Y_D(z)$ which is defined by the transformation (9). [Also note Equation (11).]

First the necessary integrations will be carried out to make algebraic the expressions involving Da, Bo, R, z, θ, and the $\{\xi_i\}$. The $\{\xi_i\}$ will then be eliminated by utilizing the approximations (41) developed in the last section. From this a simplified expression for (45) will be developed.

Evaluation of the scalar product in the numerator of (45) with the aid of the eigenequation (14) shows that

$$\int_0^1 Da\, e^{-\frac{Bo\zeta}{2}}\, U_i^{*sa}(\zeta)\, d\zeta = \int_0^1 Da\, U_i^*(\zeta)\, d\zeta = \frac{Da\, Bo\, \xi_i\, (1-R)}{\left(\xi_i^2 + \frac{Bo^2}{4}\right)} \tag{46}$$

Forms of $\psi_i^{sa}(z)$ and $U_i^{*sa}(z)$ equivalent to (15) and (16) are

$$\psi_i^{sa}(z) = \left(\frac{\xi_i}{2} - i\frac{Bo}{4}\right) e^{i\xi_i(1-z)} + \left(\frac{\xi_i}{2} + \frac{iBo}{4}\right) e^{i\xi_i(1-z)} \tag{47}$$

and

$$U_i^{*sa}(z) = \left(\frac{\xi_i}{2} - \frac{iBo}{4}\right) e^{\,i\xi_i z} + \left(\frac{\xi}{2} + \frac{iBo}{4}\right) e^{-i\xi_i z} \tag{48}$$

These two functions may be multiplied together and integrated to yield

$$\int_0^1 \psi_i^{sa}(\zeta)\, U_i^{*sa}(\zeta)\, d\zeta = \left(\frac{\xi_i}{2} - \frac{iBo}{4}\right)^2 e^{i\xi_i} + \left(\frac{\xi_i}{2} + \frac{iBo}{4}\right)^2 e^{-i\xi_i} + \left(\frac{\xi_i^2}{4} + \frac{Bo^2}{16}\right) \frac{i}{\xi_i} (e^{-i\xi_i} - e^{i\xi_i}) \tag{49}$$

Knowledge of the approximate location of the eigenvalues in the upper right quadrant of the ξ plane makes the following inequalities evident:

$$|e^{-i\xi}| >>> |e^{i\xi}| \tag{50}$$

$$\left|\frac{\xi}{2}+i\frac{Bo}{4}\right| >> \left|\frac{\xi}{2}-i\frac{Bo}{4}\right| \qquad (51)$$

Caution must be employed in the use of inequalities when discarding terms in an expression involving sums of complex numbers. Ignoring terms of small magnitude may leave an expression in which the terms of large magnitude cancel each other.

In this particular case however use of the inequality (50) to simplify (49) is an excellent approximation. Thus

$$\int_0^1 \psi_i^{sa}(z)\, U_i^{*sa}(z)\, dz \approx \left[\frac{\xi_i^2}{4}\left(1+\frac{i}{\xi_i}\right) + \frac{Bo^2}{16}\left(\frac{i}{\xi_i}-1\right) + \frac{iBo\xi_i}{4}\right] e^{-i\xi} \qquad (52)$$

It has been established in the last chapter that for every eigenvalue

$$\left|\frac{i}{\xi_i}\right| \leq \frac{1}{\dfrac{Bo}{2}+\ln R} << 1 \qquad (53)$$

For $R > e^{-Bo/6}$, use of inequality (53) to simplify (52) is quite a good approximation, since the arguments of the surviving complex terms differ by less than $\pi/2$ for the significant eigenvalues. There results

$$\int_0^1 \psi_i^{sa}(\zeta)\, U_i^{*sa}(\zeta)\, d\zeta \approx \left(\frac{\xi_i}{2}+\frac{iBo}{4}\right)^2 e^{-i\xi_i} \qquad (54)$$

This expression for the scalar product (ψ_i^{sa}, U_i^{sa}) will be used in the calculations.

The eigenfunction $\psi_i^{sa}(z)$, which stands alone in (45), may be expressed in either the form (15) or (47). At the exit of the reactor where $z = 1$

$$\psi_i^{sa}(1) = \xi_i \qquad (55)$$

When z is bounded from above by a number less than one, the following inequality is evident from the results of the last chapter

$$|e^{-i\xi(1-z)}| = e^{\hat{y}(1-z)} >> |e^{i\xi(1-z)}| = e^{-\hat{y}(1-z)} \qquad (56)$$

This inequality along with the inequality (51) indicates that the eigenfunction as written in the form (47) may be approximated by

$$\psi_i^{sa}(z) \approx \left(\frac{\xi_i}{2}+\frac{iBo}{4}\right) e^{-i\xi_i(1-z)} \quad z<1 \qquad (57)$$

Finally, η_i may be expressed in terms of ξ_i by (18).

The simplifications and manipulations (46), (54), (55), (57), and (18), may be used in the decaying function (45) to give for $R > e^{-Bo/6}$ and $z = 1$

$$Y_D(1,\theta) = 4\,Da\,Bo(1-R)\sum_i \frac{\xi_i^2 e^{i\xi_i} \exp\left[-\left(\dfrac{Bo}{4}+Da+\dfrac{\xi_i^2}{Bo}\right)\theta\right]}{\left(\xi_i-\dfrac{iBo}{2}\right)\left(\xi_i+\dfrac{iBo}{2}\right)^3\left(\dfrac{Bo}{4}+Da+\dfrac{\xi_i^2}{Bo}\right)} \qquad (58)$$

For $z < 1$ and $R > e^{-Bo/6}$

$$Y_D(z,\theta) = 2\,Da\,Bo(1-R)\sum_i \frac{\xi_i e^{i\xi_i z} \exp\left[-\left(\dfrac{Bo}{4}+Da+\dfrac{\xi_i^2}{Bo}\right)\theta\right]}{\left(\xi_i-\dfrac{iBo}{2}\right)\left(\xi_i+\dfrac{iBo}{2}\right)^2\left(\dfrac{Bo}{4}+Da+\dfrac{\xi_i^2}{Bo}\right)} \qquad (59)$$

The dependent variable $Y_D(z,\theta)$ may be converted back to the variable y_D (the negative dimensionless extent of reaction) by (9). That is, $y_D = e^{Boz/2}\, Y_D$. For each ξ_i in the upper right-quarter plane, there is a complex conjugate ξ_{i*}. Furthermore, each member of the series for $y_D(z,\theta)$ has the reflection property (22) with respect to ξ. The summations (58) and (59) must include all the $\{\xi_i\}$ with positive (or negative) real parts. This is equivalent to considering only these $\{\xi_i\}$ in the upper right quadrant and taking twice the real part of each complex member of the series. Only one of the two pure imaginary eigenvalues ξ_i should be considered, however, because they are negatives of each other and correspond to the same η_i. For purposes of computations each complex term in (58) and (59) should be put in the form

$$\hat{g}(\xi) = |\hat{g}(\xi)|\, e^{i \arg \hat{g}(\xi)}$$

Doing this and taking twice the real part gives

$$y_D(1,\theta) = 8DaBo(1-R)\sum_i \frac{|\xi_i|^2 \exp\left[\dfrac{Bo}{2}-\hat{y}_i-\left(\dfrac{Bo}{4}+Da+\dfrac{\hat{x}_i^2-\hat{y}_i^2}{Bo}\right)\theta\right]}{\left|\xi_i+\dfrac{iBo}{2}\right|\left|\xi_i-\dfrac{iBo}{2}\right|^3\left|\dfrac{Bo}{4}+Da+\dfrac{\xi_i^2}{Bo}\right|}$$

$$\times \cos\left[B(1,\theta)+\arg\xi_i-\arg\left(\xi_i+\frac{iBo}{2}\right)\right] + \text{pure imaginary contribution} \qquad (60)$$

and

$$y_D(z,\theta) = 4DaBo(1-R)\sum_i \frac{|\xi_i| \exp\left[\left(\dfrac{Bo}{2}-y_i\right)z-\left(\dfrac{Bo}{4}+Da+\dfrac{\hat{x}_i^2-\hat{y}_i^2}{Bo}\right)\theta\right]\cos B(z,\theta)}{\left|\xi_i-\dfrac{iBo}{2}\right|\left|\xi_i+\dfrac{iBo}{2}\right|^2\left|\dfrac{Bo}{4}+Da+\dfrac{\xi_i^2}{Bo}\right|}$$

$$+ \text{pure imaginary contribution} \qquad \text{for } z<1 \qquad (61)$$

where

$$B(z,\theta) = \hat{x}z - \frac{2\hat{x}\hat{y}}{Bo}\theta + \arg\xi_i - \arg\left(\xi_i-\frac{iBo}{2}\right) - 2\arg\left(\xi_i+\frac{iBo}{2}\right) - \arg\left(\frac{Bo}{4}+Da+\frac{\xi_i^2}{Bo}\right)$$

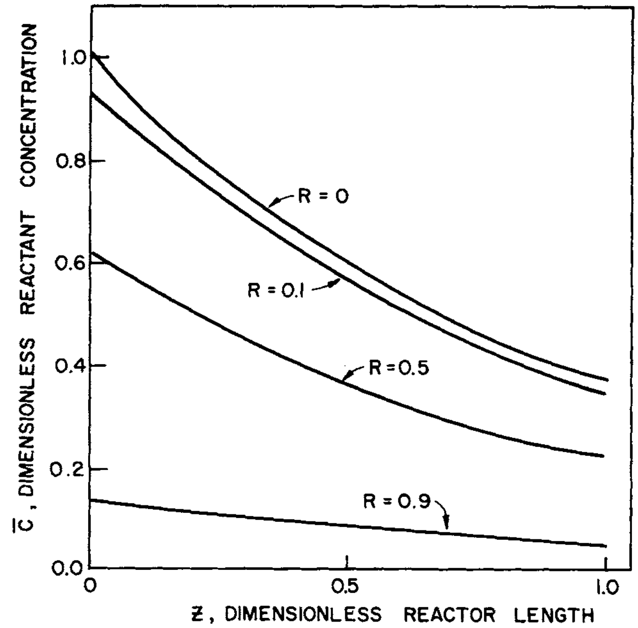

Fig. 6. Steady state concentration profiles in a tubular reactor with recycle for $Da = 1$ and $Bo = 333, 667,$ or ∞.

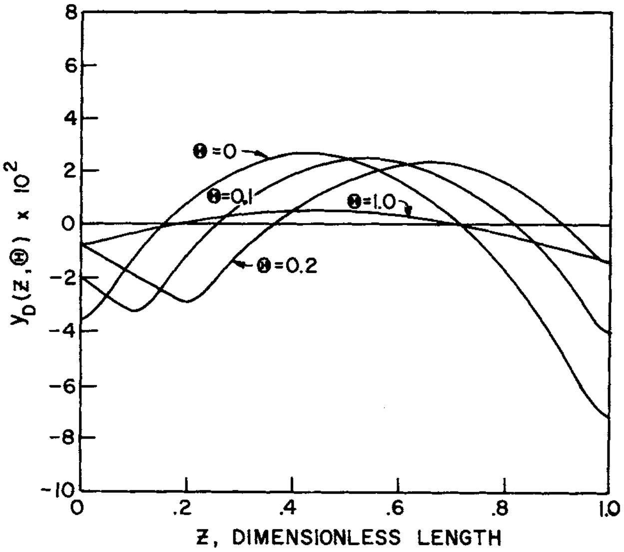

Fig. 7. Oscillating function of the steady state ($y_D(z, \theta)$ for $R = 0.5$, $Da = 1.0$, and $Bo = 666.67$. Calculated with ten terms of the approximate series. These represent waves in reactant concentration.

$$\int_0^1 \psi_i^{sa}\, U_i^{*sa}(z)\, dz \approx \frac{e^{-i\xi_i}}{4}\left(\xi_i + \frac{iBo}{2}\right)^2 \approx -\frac{Bo^2}{4}\, e^{-i\xi_i} \tag{65}$$

The resulting expression for y_D is

$$y_D(z, \theta) \approx 2Da(1-R)\, R^{(\theta - z)}\, e^{-Da\theta} \sum_{N=1}^{10} \frac{\cos\,[2\pi N(z-\theta) - \alpha_1 - \alpha_2]}{\sqrt{(4\pi^2N^2 + (\ln R)^2)(4\pi^2N^2 + (Da - \ln R)^2)}} + \frac{Da\,(1-R)R^{\theta - z}\exp\,(Da\,\theta)}{\ln R\,(\ln R - Da)} \tag{66}$$

where

$$\alpha_1 = \tan^{-1}\frac{\ln R}{2\pi N}$$

$$\alpha_2 = \tan^{-1}\frac{\ln R - Da}{2\pi N}$$

The summation of the first one hundred terms of these series, excluding the contribution from the pure imaginary eigenvalues, has been carried out with a digital computer for values of the parameters: $Bo = 666.67$, $Da = 1$, and $Da = 10$, and various values of R between 0.00001 and 0.99999. The eigenvalues were calculated by the computer by using the Newton-Raphson iterative technique. Certain of the resultant profiles are shown for various times θ in Figures 7 and 8. The contribution of either pure imaginary eigenvalue is

$$\frac{Da\,(1-R)R^{\theta-z}\exp\,(-Da\,\theta)}{\ln R\,(\ln R - Da)}$$

The smaller eigenvalues are given approximately by (41). A simpler expression for y_D results when this approximation is made in (60) and (61). Further approximations which may be made are

$$\int_0^1 Da\, e^{-Bo\zeta/2}\, U_i^{*sa}(\zeta)\, d\zeta = \frac{Da\, Bo\, \xi_i\,(1-R)}{\xi_i^2 + \dfrac{Bo^2}{4}} \approx \frac{Da\left(\dfrac{Bo}{2}\right)(1-R)}{\hat{x}_i} \tag{62}$$

$$\psi_i^{sa}(z)\, e^{Boz/2} \approx \frac{1}{2}\left(\xi_i + \frac{iBo}{2}\right)\exp\left[-i\xi_i(1-z) + \frac{Boz}{2}\right] \approx \frac{iBo}{4}\, e^{-i\xi_i}\, R^{-z}\, e^{i\hat{x}z} \tag{63}$$

$$\eta_i = \frac{Bo}{4} + Da + \frac{\xi_i^2}{Bo} \approx Da - \ln R + i\hat{x} \tag{64}$$

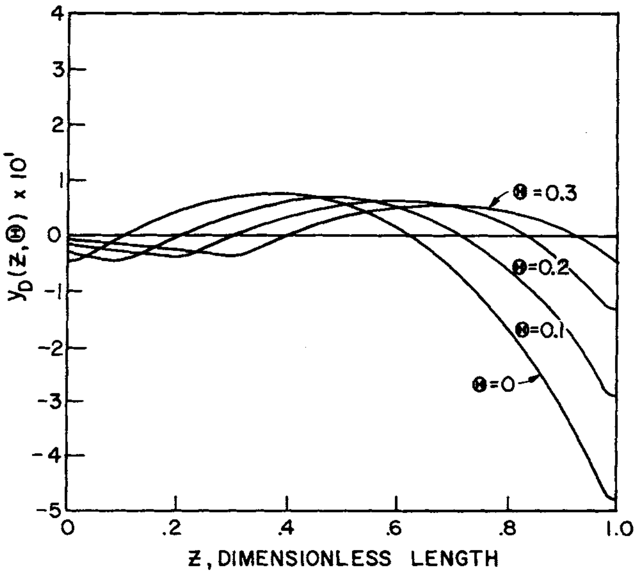

Fig. 8. Oscillating function of the steady state $y_D(z, \theta)/Da = 1.0$, for $R = 0.1$, and $Bo = 666.67$. Calculated with ten terms of the approximate series.

$$\frac{\pi}{2} \leq \alpha_2 \leq \pi, \frac{3\pi}{2} \leq \alpha_1 \leq 2\pi$$

Calculations have been made of the decaying function $y_D(z, \theta)$ by using the expression (66) with $Da = 1$, $Bo = 666.67$, and $R = 0.5$. The results agree with those calculated from the more accurate (but more complicated) expressions (60) and (61) roughly to within 2%. Only ten terms of the series for the simplified function (66) have been calculated because of the approximations involved. Convergence is fast enough that the additional ninety terms add little to the result.

Many approximations and inequalities have been used in these derivations. Necessary criteria may be loosely stated however for the existence of waves which are insensitive to the Peclet number Bo. These are that $Bo\, R \exp(Bo/2) > 2\pi$ [see Equation (33)], and that $Da/Bo < 0.05$ [this also applies to Equation (44)]. The last pertains to the dropping of the term Da in the denominators of Equations (58), (59), and (61). Furthermore, the approximations depend on Bo being large ($Bo > 10$, say).

The complete description of the function $y(z, \theta) = e^{Boz/2}\, Y(z, \theta)$ as given in (43) necessitates the evaluation of the decaying function of the initial condition

$$y_{ID}(z, \theta) = \sum_{i=0}^{\infty} \frac{\int_0^1 Y^o(z)\ U_i^{*sa}(z)\, dz}{\int_0^1 \psi_i^{sa}\ U_i^{*sa}\, dz} \psi_i^{sa}\, e^{Boz/2}\, e^{-\eta_i \theta} \tag{67}$$

y_{ID} depends on the initial condition $y^o(z) = e^{Boz/2}\, Y^o(z)$, but if this initial profile is a steady state corresponding to a different feed concentration c_{F*}, then

$$y_{ID}(z, \theta) = -\frac{c_{F*}}{c_F} y_D(z, \theta) \tag{68}$$

CONCLUSIONS

These results show that damped oscillations are induced in the reactor by a step change in feed composition. The oscillations have a wavelength approximately equal to the reactor length and they move with the interstitial velocity of the fluid. They are created by axial dispersion but are rather insensitive to the value of the diffusivity. They are superimposed upon the nonoscillatory component from the pure imaginary eigenvalues.

The moving oscillations are present because the eigenvalues have imaginary parts. When there is no recycle, the eigenvalues are constrained to be real by the Sturm-Liouville theorem and the profile sinks from the initial condition to the steady state without oscillations. Convergence is worse in this case because the eigenfunctions are like very strong exponentials, since

$$\psi_i(z) = e^{Boz/2}\, \psi_i^{sa}(z)$$

The eigenfunctions $\psi_i^{sa}(z)$ are superimposed upon $e^{Boz/2}$, a strong exponential ($Bo/2 \approx 300$ for a typical packed bed). When recycle is imposed however, $\psi_i^{sa}(z)$ becomes [see (57)]

$$\psi_i^{sa}(z) \approx \left(\frac{\xi_i}{2} + \frac{iBo}{4} \right) e^{-i\xi_i + i\xi_i z}$$

Since $\xi \approx 2\pi N + i\,(Bo/2 + \ln R)$, the real part of $e^{i\xi z}$ cancels the exponential $e^{Boz/2}$. The resultant functions $\psi_i(z)$ resemble more closely the function they are spanning when there is recycle.

ACKNOWLEDGMENT

This work was supported by the National Science Foundation.

NOTATION

Bo = Peclet number, Ul/D
c = concentration of reactant
c_o = initial concentration of reactant
c_F = feed concentration of reactant
D = diffusivity
Da = Damköhler number, kl/u
$g(\xi)$ = function whose zeroes are eigenvalues
Im = imaginary part of $g(\xi)$
k = rate constant
l = reactor length
$L(\ )$ = operator, $D\, \partial^2/\partial x^2 - u\, \partial/\partial x - k$
$\mathcal{L}(\ )$ = operator, $1/Bo\ \partial^2/\partial z^2 - \partial/\partial z$
$\mathcal{L}_a(\ )$ = adjoint of $\mathcal{L}(\ )$, $\frac{1}{Bo} \frac{\partial^2}{\partial z^2} + \frac{\partial}{\partial z}$
$\mathcal{L}^{sa}(\ )$ = operator (self-adjoint), $\frac{1}{Bo} \frac{\partial^2}{\partial z^2} - \left(\frac{Bo}{4} + Da\right)$
R = recycle ratio ($0 \leq R \leq 1$)
Re = real part of $g(\xi)$
t = time
u = interstitial fluid velocity
U_i = adjoint eigenfunction of $\mathcal{L}(\ )$
U_i^{sa} = adjoint eigenfunction of $\mathcal{L}^{sa}(\ )$
x = length coordinate
$\hat{x}$ = real part of ξ
y = dimensionless concentration, $(c - c_F)/c_F$
y_o = initial value of y
$\hat{y}$ = imaginary part of ξ
Y = dimensionless concentration function, $e^{-Boz/2}(c - c_F)/c_F$
Y_o = initial value of Y
Y_{ss} = steady state value of Y
Y_D = decaying function of Y_{ss}, $Y - Y_{ss} - Y_{ID}$
y_D = decaying function of y_{ss}, $y - y_{ss} - y_{ID}$
y_{ID} = decaying function of initial value of y, $y - y_{ss} - y_D$
z = dimensionless length, x/L
$z(Bo, R, \hat{x}, \hat{y})$ = curve in the ξ plane

Greek Letters

θ = dimensionless time, tu/l
ψ_i = eigenfunction of $\mathcal{L}(\ )$
ψ_i^{sa} = eigenfunction of $\mathcal{L}^{sa}(\ )$
η_i = eigenvalue, $Bo/4 + Da + \xi_i^2/Bo$
ξ_i = eigenvalue, $[Bo(\eta_i - Bo/4 - Da)]^{1/2}$
Γ = curve in the ξ plane

LITERATURE CITED

1. Churchill, R. V., "Complex Variables and Applications," McGraw-Hill, New York (1960).
2. ———, "Operational Mathematics," McGraw-Hill, New York (1958).
3. Coddington, E. A., and N. Levinson, "Theory of Ordinary Differential Equations," McGraw-Hill, New York (1955).
4. Danckwerts, P. V., *Chem. Eng. Sci.*, **2**, 1 (1953).
5. Hille, E., "Analytic Function Theory," Vol. I, Ginn and Co., Boston (1959).
6. Ince, E. L., "Ordinary Differential Equations," Dover, New York (1956).
7. Lapidus, Leon, "Digital Computation for Chemical Engineers," McGraw-Hill, New York (1962).
8. Newman, H. H., and R. C. Bennett, *Chem. Eng. Progr.*, **55**, 65 (1959).
9. Schmeal, W. R., Ph.D. thesis, Univ. Minnesota, Minneapolis (1965).
10. Wylie, C. R., Jr., "Advanced Engineering Mathematics," McGraw-Hill, New York (1960).

Manuscript received July 20, 1966; paper accepted September 16, 1966.